

## Hopping over a heat barrier

Anja Garber, Nicholas R. Moloney, and Holger Kantz

*Max Planck Institute for the Physics of Complex Systems, Nöthnitzer Strasse 38, D 01187 Dresden, Germany*

(Received 16 September 2010; revised manuscript received 8 December 2010; published 28 March 2011)

We analyze diffusion in a finite domain with a position-dependent diffusion coefficient in terms of a stochastic hopping process. Via a coordinate transformation, we map the original system onto a problem with constant diffusion but nontrivial potential. In this way we show that a regime with enhanced diffusion acts as a potential barrier. We compute first-passage time distributions, hopping rates, and eigenvalues of the Fokker-Planck operator, and thereby verify that diffusion with a heat barrier is equivalent to a hopping process between metastable states.

DOI: [10.1103/PhysRevE.83.031134](https://doi.org/10.1103/PhysRevE.83.031134)

PACS number(s): 05.40.-a, 05.10.Gg, 02.50.Ey

### I. INTRODUCTION

The motion of a particle in a bistable system subject to noise is one of the best studied of all stochastic processes. This is motivated by the enormous range of applications in all fields of science including electronics (switching in tunnel diode circuits [1]), chemical physics (dynamics of the Schlögl reaction [2]), cellular biology (bistability in gene expression [3]), laser physics (switching in a two-mode laser [4]), climatology (tipping points in climate change [5]), and condensed-matter physics (electrical bistability in polymers [6]), to name just a few examples. One of the central problems in such studies is the estimation of time scales for the metastable states. Following Kramers [7], techniques for tackling this calculation have evolved and are summarized in numerous textbooks [8–10]. More recently, analyses have been specialized to include, for example, multiplicative noise [11], Lévy noise [12], and periodic driving [13].

However, all of the above cited work refers to systems where the deterministic forces are the cause of multistability. There have been some discussions on noise-induced bistability, for example, in superfluids [14] or surface waves [15], but there nonlinearity of the deterministic forces and the vicinity of bifurcations are needed to bring about the multistability. Very sporadically, the literature reports on noise-induced bistability and/or noise-induced bimodality, where it is the noise and not the deterministic forces that causes the loss of stability of a single equilibrium point. This has been reported particularly in atmospheric physics, e.g., Refs. [16] and [17], and in astrophysics [18]. In this and many of the aforementioned work, no distinction is made between bimodality of some invariant distribution and bistability of the dynamics.

It is, however, physically essential whether a system is bistable or whether its probability density is simply bimodal. If a trajectory in a finite domain oscillates systematically between left and right, the probability density will be related to the inverse of the velocity, and a bimodal distribution can be easily generated by speeding up the trajectory in the center of the domain. This is very different from bistability. In the latter, the trajectory would tend to stay for some time in one domain, and then jump into another one. More specifically, the relaxation toward local equilibrium inside one domain should be much faster than the convergence toward the relative balance between the different metastable states.

In this paper we are concerned with systems whose deterministic part supports a single stable equilibrium point only,

and which, under the influence of multiplicative noise, exhibit a bimodal distribution. We want to understand whether the existence of such a bimodal distribution is indeed synonymous with bistability of the noisy dynamics.

We restrict our discussion to Markov processes in real time and with real-valued variables, i.e., to systems described by Langevin-like equations and their corresponding Fokker-Planck formulations. Individual sample paths are initial value solutions of these stochastic differential equations, where details of the trajectory depend on the chosen realization of the noise. In contrast, their corresponding Fokker-Planck equations are deterministic partial differential equations of the form

$$\frac{\partial}{\partial t} \rho(x, t) = \left[ -\frac{\partial}{\partial x} F(x) + \frac{\partial^2}{\partial x^2} D(x) \right] \rho(x, t) \quad (1)$$

in one dimension (1D), with drift  $F(x)$  and diffusion  $D(x)$ , which describe the time evolution of smooth probability densities.

The asymptotic state, the invariant density, can be given in closed form in the 1D case as

$$\rho_0(x) = \frac{N_0}{D(x)} \exp \left\{ \int_{-\infty}^x \frac{F(x')}{D(x')} dx' \right\}, \quad (2)$$

where  $N_0$  is a normalization constant. This density reflects an equilibrium property of the process: It quantifies the probability to find a trajectory in a given subset of the phase space, averaged over initial conditions and noise realizations. Although the shape of the invariant density depends on the deterministic and stochastic forces of the process, it is a static quantity.

In many situations, dynamical properties are of interest. When specifying a domain of initial conditions and another target domain, a typically sought-after quantity is the mean of the times individual trajectories need, under the joint action of deterministic and stochastic forces, to pass from the initial condition into the target domain, or its inverse: the hopping rate. A more refined way to present this information is through the probability distribution of first-passage times.

Hopping rates are a natural concept if the stochastic process has two or more metastable states and rare transitions between them. In 1D problems with constant noise amplitude  $\sqrt{D}$ , the Kramers rate is a useful approximation in the low-noise regime: Let the deterministic force be the negative gradient of the potential  $U(x)$  (which always exists for 1D problems),

and let the second derivative of  $U(x)$  exist, then the Kramers escape rate out of a potential well with a minimum at  $x = 0$  over a barrier with a maximum at  $x = a$  reads

$$r_K = \frac{1}{2\pi} \sqrt{-U''(0)U''(a)} e^{-[U(a)-U(0)]/D}. \quad (3)$$

In this paper, however, we consider 1D processes with a state-dependent noise amplitude, sometimes called multiplicative noise, without any bistability of the deterministic force. For the particularly simple case of vanishing drift terms  $F(x)$  and state-dependent diffusion  $D(x)$ , one can easily see from Eq. (2) that state-dependent diffusion can shape the probability density in a similar way to deterministic drift. One example is the case  $F(x) = 0$  and  $D(x) = \exp(x^2)$ , having Gaussian invariant density. Other solvable examples exist in the literature for certain diffusion profiles, e.g., Refs. [19] and [20], while the calculation of an effective diffusion constant is discussed in Ref. [21].

In Ref. [22] it was emphasized that a bimodal invariant density does not necessarily require a deterministic double-well potential, but that it might as well arise in a single-well potential with state-dependent diffusion. The issue that we investigate here is whether such a bimodal distribution owing to multiplicative noise implies that it is justified to consider the underlying process as a hopping process between metastable states, even if the usual concepts such as the Kramers rate are not readily applicable. To this end, we study how regions with large diffusion coefficients influence relaxation properties in the absence of any deterministic forces.

After introducing the model in Sec. II, we compute the first-passage time distribution and its mean in Sec. III, where we transform the original model onto a model with constant diffusion coefficient but nontrivial potential. In Sec. IV we compute eigenvalues and eigenstates of the Fokker-Planck equation and verify the existence of a gap in the spectrum, showing that our model process is indeed bistable.

## II. THE MODEL

We consider diffusion on an interval with reflecting walls, without any deterministic force, but with a position-dependent diffusion coefficient. More specifically, the diffusion will be piecewise constant with a high value in some central domain, called the “hot” domain, and a smaller value outside this domain, called the “cold” parts for brevity.

For the purpose of analytical calculations, we introduce a linear interpolation of width  $\epsilon/2$  between the two different diffusion levels to make the diffusion coefficient continuous. Taking the limit  $\epsilon \rightarrow 0$  recovers the results of the discontinuous system. The resulting diffusion coefficient is given by

$$D(x) = \begin{cases} D_1 & \text{if } \frac{L_2+\epsilon}{2} < |x| < \frac{L_1+L_2+\epsilon}{2}, \\ \frac{(D_2-D_1)(L_2-2|x|)+\epsilon D_2}{\epsilon} & \text{if } \frac{L_2}{2} < |x| < \frac{L_2+\epsilon}{2}, \\ D_2 & \text{if } |x| < \frac{L_2}{2}, \end{cases} \quad (4)$$

as illustrated in Fig. 1. The invariant density of this process, as given by Eq. (2), is proportional to the inverse of the diffusion coefficient,  $\rho_0(x) \propto 1/D(x)$ , which is a bimodal distribution.

Figure 2 shows two sample paths of the discontinuous system ( $\epsilon = 0$ ), one resulting from free diffusion, i.e.,  $D_1 = D_2$  (upper panel), and one from diffusion constants

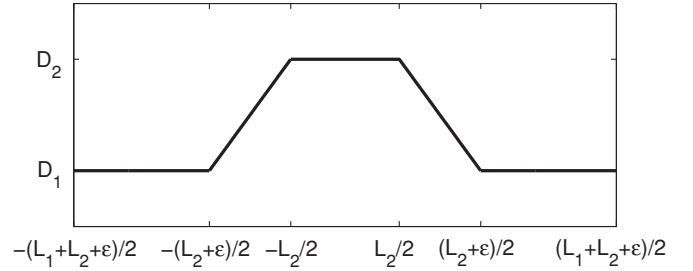


FIG. 1. Illustration of the model system, showing the state dependence of the diffusion coefficient with linear interpolation.

$D_2 = 20D_1$  (lower panel). It is clearly visible that the strong diffusion in the middle of the system introduces hopping dynamics, in which the sample path resides in the outer parts of the system most of the time, with rapid crossing through the middle regime.

A sample path that represents the same bimodal invariant density, but having very different temporal correlations, is shown in Fig. 3, consisting of so-called surrogate data [23], i.e., a scrambled version of the time-discrete path of Fig. 2(b). Random scrambling of the original sequence  $x(t)$  yields a sequence of identically and independently distributed random variables. Its continuous time limit would be white noise with a non-Gaussian probability density. (Combining successive data points by lines as in Fig. 3 represents a process with nonvanishing autocorrelations on time lags smaller than the

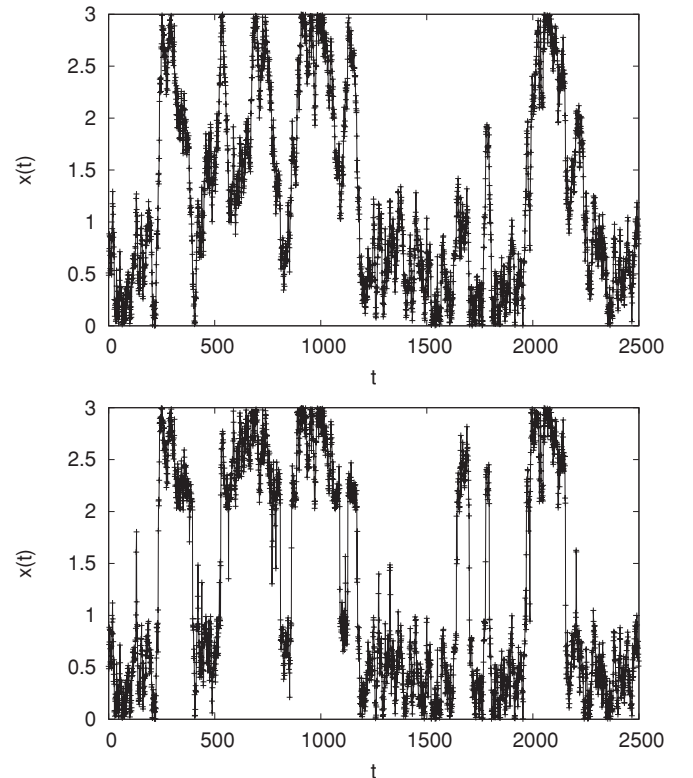


FIG. 2. Sample paths for the fully discontinuous model system ( $\epsilon = 0$ ) with diffusion constants  $D_1 = D_2 = 1$  (upper panel) and  $D_1 = 1$  and  $D_2 = 20$  (lower panel). The higher diffusion regime in this simulation extends from  $x = 1$  to  $x = 2$ .

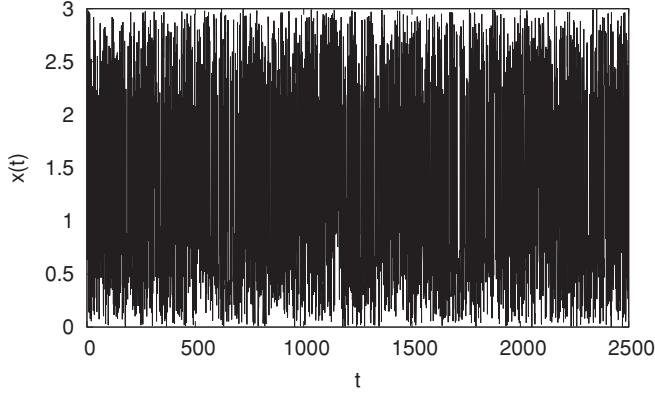


FIG. 3. A path generated by linear interpolation of the randomly scrambled data of Fig. 2(b).

sampling interval and is therefore not the illustration of white noise, because the sample paths of white noise are nowhere continuous.) It is evident that, despite the bimodality of the probability density function, such a process would not be called a “hopping process”: there is no time-scale separation between the motion inside the highly populated areas and the motion across the sparsely populated central domain. Therefore, visual inspection of the contrast between Figs. 2 and 3 clearly suggests that the considered diffusion process does indeed have properties of metastability and hopping.

In the next section we will derive analytical results for a hopping rate to further clarify whether this situation defines a process that may indeed be called “hopping over a heat barrier.”

### III. TRANSFORMATION TO A PROBLEM WITH CONSTANT DIFFUSION COEFFICIENT

Because analytical results for the mean first-passage time are much easier to derive for systems with additive noise, we make use of the transformation of variables [8] given by Eq. (5), which changes the system from multiplicative noise with a diffusion coefficient  $D(x)$  to a constant diffusion  $\tilde{D} = 1$ :

$$y = \int_c^x \frac{dx'}{\sqrt{D(x')}}}, \quad (5)$$

where  $c$  is an arbitrary constant.

The drift  $\tilde{F}$  in the transformed system will then be given by

$$\tilde{F}(x) = \frac{1}{\sqrt{D(x)}} \left[ F(x) - \frac{1}{2} \frac{d}{dx} D(x) \right]. \quad (6)$$

As the coordinate transformation is a rescaling of only the space coordinates, not of time, the transition rate of the transformed process is identical to the transition rate of the original process.

Applying the transformation to our model system and choosing the constant  $c$  such that the system is symmetric around  $y = 0$  leads to the following potential in the new coordinate system [with the same subdivision of the system as in Eq. (4)]:

$$U(y) = \begin{cases} 0, \\ \log \left| |y| - \frac{L_2}{2\sqrt{D_2}} - \frac{\epsilon\sqrt{D_2}}{D_2 - D_1} \right| - \log \left| \frac{\epsilon\sqrt{D_1}}{D_2 - D_1} \right|, \\ \log \sqrt{\frac{D_2}{D_1}}. \end{cases} \quad (7)$$

Hence, the transformed problem is a stochastic motion with a constant diffusion coefficient in a finite domain with reflecting boundaries and a potential barrier in the center, if  $D_2 > D_1$ . In the limit  $\epsilon \rightarrow 0$ , i.e., in the problem without linear ramps in  $D(x)$ , the potential is piecewise constant. The height of the barrier is given by  $\log \sqrt{D_2/D_1}$  and hence is higher the stronger the diffusion in the center. What is concealed is the fact that in the transformed  $y$  coordinates, the width of the barrier is given by  $L_2/\sqrt{D_2}$  and is therefore smaller, the larger  $D_2$ . Altogether, in the  $y$  coordinates, this problem is a conventional hopping process between two metastable states across a potential barrier.

Because the coordinate transformation leads to a problem with a well-defined potential and constant diffusion  $D$ , the mean first-passage time  $T$  from a starting point  $x_0$  in the left-hand well to an endpoint at  $x_e$ , given a reflecting wall at  $a = -(L_1 + L_2)/2$ , i.e., at the left-hand boundary of the system, can be calculated in closed form [10]:

$$T(x_0 \rightarrow x_e) = \frac{1}{D} \int_{x_0}^{x_e} dy \exp \left[ \frac{U(y)}{D} \right] \times \int_a^y dz \exp \left[ -\frac{U(z)}{D} \right]. \quad (8)$$

This formula provides the usual starting point for a Kramers approximation that decouples the double integral through a parabolic ansatz for the potential near its extrema. In the case of our model system, however, the extrema are degenerate because the potential is piecewise constant. The Kramers approximation is therefore not applicable even in the transformed coordinates.

However, because in this special case the double integral can be calculated exactly, an approximation proves unnecessary, and the mean first-passage time (after transforming the space coordinates back to the original coordinate system) is given by

$$T(x_0 \rightarrow x_e) = \frac{L_1^2}{8D_1} - \frac{(2x_0 + L_1 + L_2)^2}{8D_1} + \frac{L_1(2x_e + L_2)}{4D_1} + \frac{1}{2D_2} \left( x_e + \frac{L_2}{2} \right)^2 \quad (9)$$

if  $x_e \in [-L_2/2, L_2/2]$ , and by

$$T(x_0 \rightarrow x_e) = \frac{L_1^2}{8D_1} - \frac{(2x_0 + L_1 + L_2)^2}{8D_1} + \frac{L_1 L_2}{2D_1} + \frac{L_2^2}{2D_2} + \sqrt{\frac{D_1}{D_2}} \frac{(L_1 D_2 + 2L_2 D_1)(2x_e - L_2)}{4D_1 D_2} + \frac{(2x_e - L_2)^2}{8D_1} \quad (10)$$

if  $x_e > L_2/2$ .

The passage times for  $x_0 < -L_2/2$  and  $x_e = L_2/2$  hereby characterize what we would like to call “hopping” from left to right: paths from the left cold domain through the hot central part into the right cold domain. In this case, Eqs. (9) and (10) are identical. Whereas the first two terms describe the average time needed to arrive at the transition point  $-L_2/2$ , the third and fourth together give the time needed to pass through the

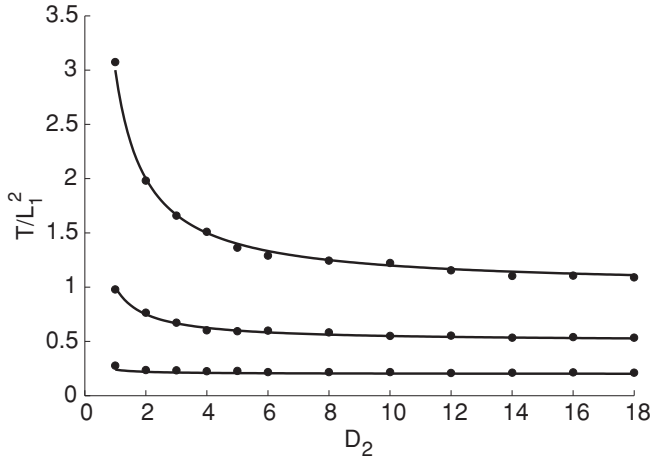


FIG. 4. Mean first-passage times as a function of the diffusion coefficient  $D_2$  for different values of the width of the hot region  $L_2$  (from top to bottom:  $L_2/L_1 = 2, 1, 0.4$ ). Symbols: Numerical average from one long trajectory ( $10^8$  time steps); continuous lines: Eq. (9) with  $x_0 = -L_2/2$  and  $x_e = L_2/2$ .

“hot” region, including the possibility that the path returns into the “cold” region before arriving on the right-hand side.

Figure 4 illustrates the dependence of this mean first-passage time on the parameters  $D_2$  and  $L_1/L_2$ . It also includes the numerically determined values taken from one long trajectory to compare for accuracy. The value of the diffusion constant in the “cold” domains was chosen as  $D_1 = 1$  throughout this paper, because varying the second diffusion constant in addition to  $D_2$  only leads to an overall rescaling of time. Numerical integration was done with a simple Euler-Mayurama scheme. The reflecting boundary conditions at  $-(L_1 + L_2)/2$  were implemented by mirroring back a trajectory inside  $[-(L_1 + L_2)/2, (L_1 + L_2)/2]$  when it leaves this interval, but no corrections were employed at  $-L_2/2$  or  $L_2/2$  (where the diffusion coefficient changes its value) in order to conserve detailed balance.

As can clearly be seen in Fig. 4, the passage time increases when the central region gets broader and it decreases when the diffusion coefficient in this region is increased. This result does not come as a surprise, as the traversing of a larger distance should take more time, and an increased diffusion coefficient accelerates the dynamics. It does, however, seem to contradict the idea that a regime of enhanced diffusion might act as a barrier. On the other hand, when considering the transformed system, we can see that although the potential barrier increases with  $D_2$ , its width decreases, so that the passage time can indeed decrease with increasing  $D_2$ .

In fact, as described in the Appendix, it is possible to obtain not only the mean first-passage time exactly, but also the full first-passage distribution (for the case  $\epsilon = 0$ ) by numerically inverting its analytical Laplace-space solution (see Fig. 5). The evolution of the distributions with increasing  $D_2$  is in keeping with the decreasing mean first-passage times shown in Fig. 4. The cutoffs at short and long times, visible in the log-log inset, are essentially set by the time scales for diffusing from the initial starting point to the absorbing boundary, and from the reflecting boundary to the absorbing boundary, respectively.

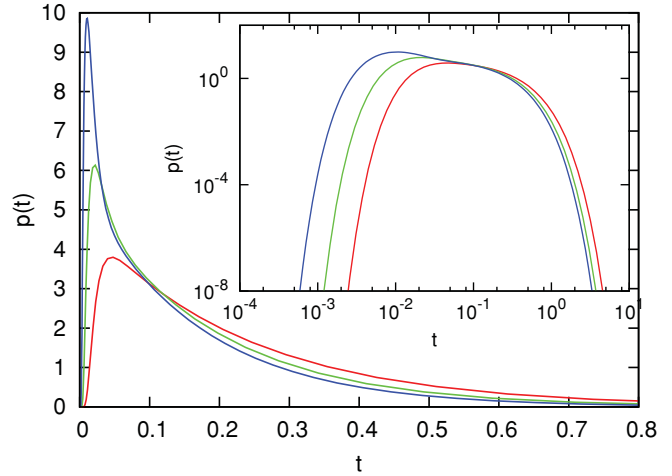


FIG. 5. (Color online) First-passage time distributions  $p(t)$  from  $x_0 = -L_2/2$  to  $x_e = L_2/2$  for  $L_1/L_2 = 1$  and  $D_2 = 4, 2, 1$  (top to bottom at small values). Inset:  $p(t)$  on a log-log scale.

#### IV. EIGENVALUES OF THE FOKKER-PLANCK OPERATOR AND RELAXATION

Despite the fact that the transformed problem resembles a typical hopping problem, the decrease of the mean first-passage time under an increase of  $D_2$  does not really conform with the initial assumption of enhanced diffusion acting as a barrier. We therefore analyze the eigenvalues of the Fokker-Planck operator of this problem.

If we interpret an initial probability density  $\rho_i$  as a linear combination of the right eigenfunctions  $\rho_k$  of the Fokker-Planck operator  $\mathcal{F}$ , with  $\mathcal{F}\rho_k = -\lambda_k\rho_k = \dot{\rho}_k$ , then we see that the smallest nonzero eigenvalue  $\lambda_1$  controls the relaxation of a generic initial density toward the invariant density  $\rho_0$ . The existence of a metastable state is usually assumed if this first nontrivial eigenvalue is much closer to 0 than is the difference between the first and the second eigenvalue. This is formalized in the theory of Markov processes: A system is called bistable only if there is one nontrivial eigenvalue close to unity that is separated from the other (smaller) eigenvalues by a gap [24].

For the special case in which the hot and cold domains are exactly equal in length (in the transformed coordinates), analytical results are given in Ref. [8] for the eigenvalues and eigenfunctions. However, for general  $L_1$  and  $L_2$ , a transcendental equation has to be solved. Because this makes numerical calculations necessary anyhow, we take the eigenvalues directly from the simulated paths of this system.

To this end, we introduce a rather fine partition of the range  $[-(L_1 + L_2)/2, (L_1 + L_2)/2]$  and determine a transition matrix  $M_{ij}$  by numerical simulations: We simply count the number of occurrences of a situation where the trajectory is in bin  $i$  at time  $t$  and in bin  $j$  at time  $t + \Delta t$  for suitably small  $\Delta t$ . This is a numerical estimate of  $\exp(\Delta t \mathcal{F})$ . The logarithms of its eigenvalues, divided by  $\Delta t$ , are therefore a good approximation of the eigenvalues of the Fokker-Planck operator. Because  $M_{ij}$  by construction is a Markov matrix, its leading eigenvalue is unity, which translates into the eigenvalue 0 of the Fokker-Planck operator corresponding to the invariant density.



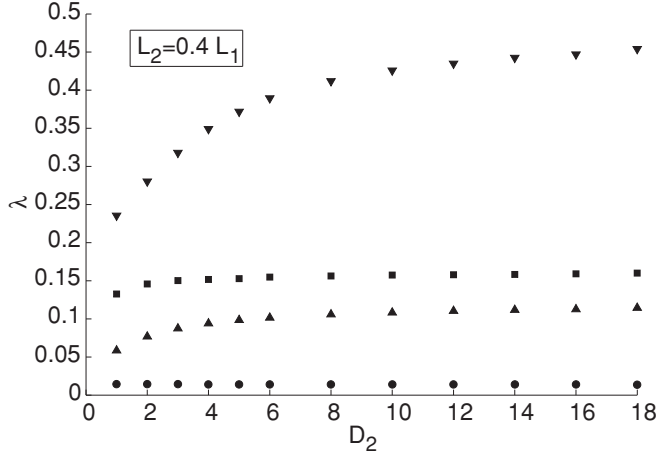


FIG. 6. Dependence of the first four nontrivial eigenvalues (bottom to top) of the Fokker-Planck operator obtained from the transition matrix  $M_{ij}$  on the diffusion constant  $D_2$  of the hot domain for a ratio of domain lengths  $L_2/L_1 = 0.4$ .

The numerically obtained invariant density is of course not precisely a piecewise constant but has smooth transitions at the borders between hot and cold regions, whose width is controlled by the temporal step width. Despite these inaccuracies, the error in terms of eigenvalues is negligible,

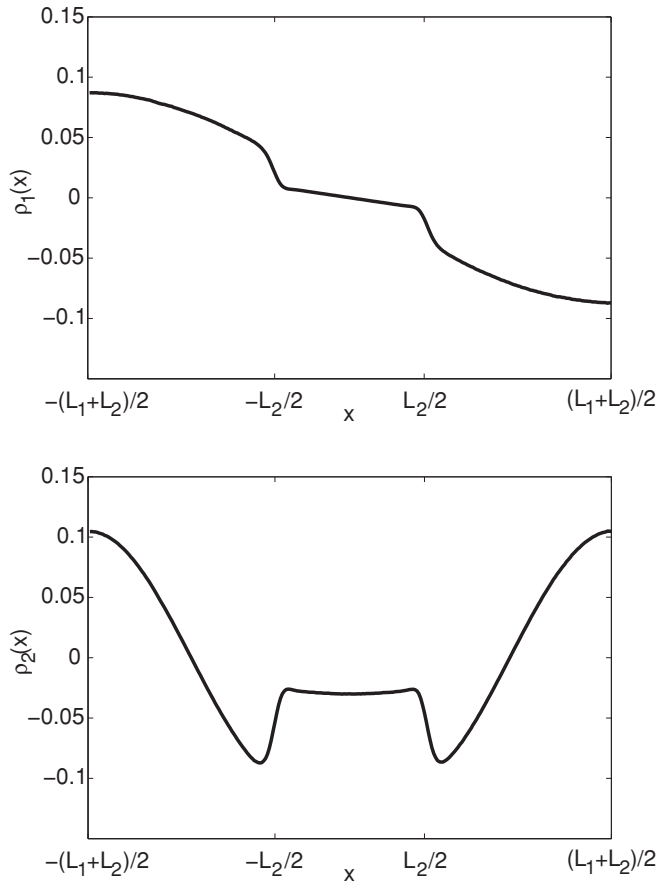


FIG. 7. First (upper panel) and second (lower panel) eigenfunction of the Fokker-Planck operator for the discontinuous system ( $\epsilon = 0$ ) with a ratio of domain lengths  $L_2/L_1 = 0.4$  and  $D_2 = 4$ .

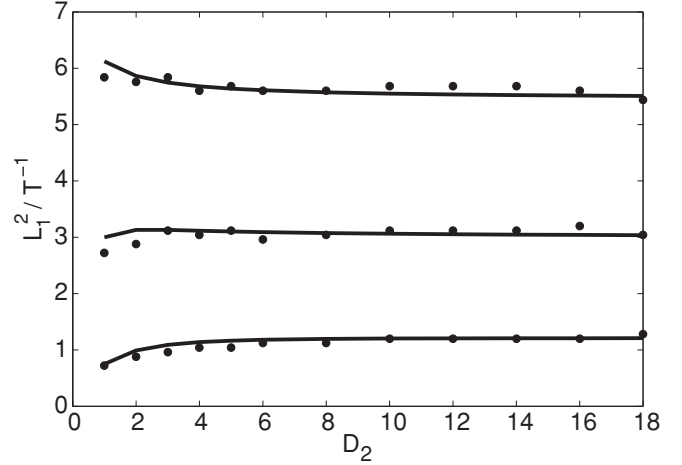


FIG. 8. Inverse mean first-passage time to  $x_e = 0$  from initial conditions averaged over  $-(L_1 + L_2)/2 < x_0 < 0$  as a function of  $D_2$  for  $L_2/L_1 = 0.4, 1.3$  (continuous lines from top to bottom), and first nontrivial eigenvalues of the Fokker-Planck operator for the same values of  $L_2/L_1$  (circles).

and the general agreement between numerics and analytical results is good (as seen already in Fig. 4).

In Fig. 6 we plot the first four nontrivial eigenvalues of the Fokker-Planck operator versus  $D_2$  for  $L_2/L_1 = 0.4$ . We see that there is indeed a gap between the first and second eigenvalue, which increases with  $D_2$ , indicating metastability that grows with barrier height.

In Fig. 7 we plot the corresponding two eigenfunctions for  $L_2/L_1 = 0.4$  and  $D_2 = 4$  (the qualitative behavior is independent of these values while  $D_1 < D_2$ ). The first eigenfunction is antisymmetric with respect to the middle of the system, showing that it is related to the imbalance between the weight of the right and left cold domains. The second eigenfunction, in contrast, has antisymmetric parts within the cold wells and is thus more related to the equilibration within the wells.

To confirm these interpretations, Fig. 8 compares the first nontrivial eigenvalue as an estimate of the hopping rate between the wells to the inverse of the mean first-passage times computed analytically as outlined in Sec. III, finding good agreement. Note, however, that the eigenfunction is antisymmetric with respect to the middle of the hot domain, i.e., to  $x = 0$ , and the rate described by its eigenvalue therefore has to be compared to the mean first-passage time to  $x_e = 0$  starting from averaged initial conditions in the region  $-(L_1 + L_2)/2 < x_0 < 0$ .

As mentioned in the Appendix, the time-dependent relaxation toward the invariant density is available exactly by numerically inverting the analytical Laplace-space solution. This allows us to visually confirm the notions of metastability discussed above. Figure 9 shows the relaxation of a  $\delta$ -peak initial condition  $\rho(x, 0) = \delta(x + [L_1/2 + L_2]/2)$  centered in the middle of the left well. It is apparent that relaxation within a well (i.e., convergence to a uniform density profile) is on a faster time scale as compared to the transfer of probability mass between the left and right wells. Indeed, in the sequence of densities shown, only by the third time

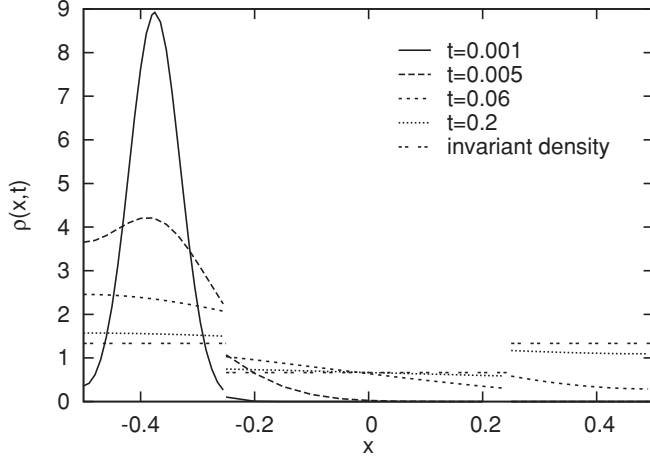


FIG. 9. Relaxation of a  $\delta$ -peak initial condition centered in the middle of the left well (where time increases from top to bottom) toward the invariant density, with  $L_1/L_2 = 1$ ,  $D_2 = 2$ .

update does any significant probability mass appear in the right well.

## V. CONCLUSIONS

The literature on state-dependent noise amplitudes, which is generally called multiplicative noise, is very rich. While theoretical investigations have discussed scenarios such as noise-induced phase transitions, in more applied research the formation of bimodal distributions or bistability has been reported only sporadically. A clear distinction between bimodal distributions and bistability of a system has not been established despite the marked physical differences between the two.

Our investigation of a very simple model system shows that a domain of enhanced diffusion in a 1D stochastic process acts as a potential barrier, thereby forming metastable states and giving rise to hopping processes. By transforming the original problem onto one with a state-independent diffusion coefficient, we demonstrate the equivalence with a potential barrier. Although the dependence of the first-passage time on the strength of diffusion  $D_2$  seems to contradict this point of view, an analysis of the eigenvalues (the correctness of its interpretation being verified by studying the relaxation of  $\delta$  densities) shows the separation of time scales, and the corresponding eigenfunctions confirm that indeed the exchange between the two cold domains is suppressed by the hot domain in between.

Our model system has a very simple and intuitive physical analog: Consider a box filled with air, which is held at a given temperature through contact with the walls of the container. The container is subdivided by a narrow domain of local heating, e.g., by radiation. Thereby, the local temperature of the air is higher, and thus the diffusion of gas molecules is enhanced. Our results now predict that the transport across this hot air regime (ignoring convection) is much slower than the relaxation inside each cold regime. Therefore, a release of pollutants at some spot in one cold domain will very quickly pollute the domain in which it was released homogeneously,

and diffuse only slowly over the high-diffusion barrier into the other domain.

Summarizing, we have confirmed that state-dependent diffusion, or multiplicative noise, cannot only give rise to multimodal distributions, but that the dynamics is really a hopping process between metastable states, even if the deterministic potential has a single well only.

## APPENDIX

Although we are not able to solve the time-dependent diffusion problem given by Eqs. (1) and (4) directly, a solution nevertheless exists in Laplace space:

$$\rho(x,s) = \int_0^\infty dt e^{-st} \rho(x,t). \quad (\text{A1})$$

Following the presentation in Ref. [25], the Laplace transform of the diffusion equation reads

$$s\rho(x,s) - \delta(x - x_0) = \frac{\partial^2}{\partial x^2} D(x)\rho(x,s), \quad (\text{A2})$$

with an initial condition  $\rho(x,t=0) = \delta(x - x_0)$ . For the problem with a top-hat diffusion profile, Eq. (A2) can be written with a uniform diffusion constant in the three regions  $[-(L_1 + L_2)/2, -L_2/2]$ ,  $[-L_2/2, L_2/2]$ ,  $[L_2/2, (L_1 + L_2)/2]$  separately, with  $x_0 \in [-(L_1 + L_2)/2, -L_2/2]$ . In the latter two regions, Eq. (A2) is homogeneous, while in the first region it is homogeneous on either side of  $x = x_0$ . Thus, the continuity conditions read

$$\rho(x,s)|_{x \uparrow x_0} = \rho(x,s)|_{x \downarrow x_0}, \quad (\text{A3})$$

$$\rho'(x,s)|_{x \downarrow x_0} - \rho'(x,s)|_{x \uparrow x_0} = -1/D_1, \quad (\text{A4})$$

$$D_1 \rho(x,s)|_{x \uparrow -L_2/2} = D_2 \rho(x,s)|_{x \downarrow -L_2/2}, \quad (\text{A5})$$

$$D_1 \rho'(x,s)|_{x \uparrow -L_2/2} = D_2 \rho'(x,s)|_{x \downarrow -L_2/2}, \quad (\text{A6})$$

$$D_2 \rho(x,s)|_{x \uparrow L_2/2} = D_1 \rho(x,s)|_{x \downarrow L_2/2} \quad (\text{A7})$$

$$D_2 \rho'(x,s)|_{x \uparrow L_2/2} = D_1 \rho'(x,s)|_{x \downarrow L_2/2}, \quad (\text{A8})$$

where Eq. (A4) is the result of integrating Eq. (A2) around a small region including  $x = x_0$ . In addition, two conditions are provided by the appropriate boundary conditions at  $x = \pm(L_1 + L_2)/2$ . This completes the specification of the problem. The solutions within the different regions are expressible as linear combinations of  $\exp(\pm\sqrt{s/D_{1,2}})$ .

For the case of studying relaxation of an initial  $\delta$  peak toward the invariant density, reflecting conditions are imposed at  $x = \pm(L_1 + L_2)/2$ . For the Laplace-transformed first-passage time distribution  $p(s)$ , meanwhile, absorbing boundary conditions are imposed at  $x = x_e$  (or at whichever point first passage is sought), by which

$$p(s) = -D_{1,2} \left. \frac{\partial}{\partial x} \rho(x,s) \right|_{x=x_e}, \quad (\text{A9})$$

which is nothing other than the exit current at  $x = x_e$ . Because  $p(s)$  is the moment-generating function for the first-passage

time distribution  $p(t)$ , the mean first-passage time is given by

$$T(x_0 \rightarrow x_e) = - \left. \frac{\partial}{\partial s} p(s) \right|_{s=0}. \quad (\text{A10})$$

The resulting expressions for  $\rho(x,s)$  and  $p(s)$  are too cumbersome to reproduce here, and an analytical inversion is not available. However, using *Mathematica* and the numerical inversion algorithm provided by Valkó and Abate [26],  $\rho(x,t)$  and  $p(t)$  can be obtained to very high precision.

- 
- [1] R. Landauer, *J. Appl. Phys.* **33**, 2209 (1962).  
 [2] F. Schlögl, *Phys. Rep.* **62**, 267 (1980).  
 [3] J. Z. Kelemen, P. Ratna, S. Scherrer, and A. Becskei, *PLoS Biol.* **8**, e1000332 (2010).  
 [4] R. Roy, R. Short, J. Durnin, and L. Mandel, *Phys. Rev. Lett.* **45**, 1486 (1980).  
 [5] T. M. Lenton, H. Held, E. Kriegler, J. W. Hall, W. Lucht, S. Rahmstorf, and H. J. Schellnhuber, *Proc. Natl. Acad. Sci. USA* **105**, 1786 (2008).  
 [6] J. Ouyang, C.-W. Chu, C. R. Szmanda, L. Ma, and Y. Yang, *Nat. Mater.* **3**, 918 (2004).  
 [7] H. A. Kramers, *Physica* **7**, 284 (1940).  
 [8] H. Risken, *The Fokker-Planck Equation*, ed. (Springer, Berlin, 1996).  
 [9] N. G. van Kampen, *Stochastic Processes in Physics and Chemistry* (North Holland, Amsterdam, 1992).  
 [10] C. W. Gardiner, *Handbook of Stochastic Methods for Physics, Chemistry, and the Natural Sciences*, ed. (Springer, Berlin, 2004).  
 [11] Y. Hasegawa and M. Arita, *Physica A* **389**, 4450 (2010).  
 [12] B. Dybiec, E. Gudowska-Nowak, and P. Hänggi, *Phys. Rev. E* **75**, 021109 (2007).  
 [13] P. Talkner, L. Machura, M. Schindler, P. Hänggi, and J. Luczka, *New J. Phys.* **7** (2005).  
 [14] D. Griswold and J. T. Tough, *Phys. Rev. A* **36**, 1360 (1987).  
 [15] S. Residori, R. Berthet, B. Roman, and S. Fauve, *Phys. Rev. Lett.* **88**, 024502 (2001).  
 [16] P. Sura, *J. Atmos. Sci.* **59**, 97 (2002).  
 [17] D. Entekhabi, I. Rodriguez Iturbe, and R. Bras, *J. Climate* **5**, 798 (1992).  
 [18] F. Spahn, A. Krivov, M. Sremcevic, U. Schwarz, and J. Kurths, *J. Geophys. Res.* **108**, 5021 (2003).  
 [19] D. ben Avraham, S. Redner, D. B. Considine, and P. Meakin, *J. Phys. A* **23**, L613 (1990).  
 [20] D. ben Avraham, D. Considine, P. Meakin, S. Redner, and H. Takayasu, *J. Phys. A: Math. Gen.* **23**, 4297 (1990).  
 [21] S. Revathi and V. Balakrishnan, *J. Phys. A* **26**, 5661 (1993).  
 [22] P. Sura, M. Newman, C. Penland, and P. Sardeshmukh, *J. Atmos. Sci.* **62**, 1391 (2005).  
 [23] J. Theiler, S. Eubank, A. Longtin, B. Galdrikian, and J. D. Farmer, *Physica D* **58**, 77 (1992).  
 [24] M. Dellnitz and O. Junge, *SIAM J. Numer. Anal.* **36**, 491 (1999).  
 [25] S. Redner, *A Guide to First-Passage Processes* (Cambridge University Press, Cambridge, UK, 2001).  
 [26] P. P. Valkó and J. Abate, *Comput. Math. Applic.* **48**, 629 (2004).